



A circular economy use of waste wood sawdust for wood plastic composite production: effect of bio-plasticiser on the toughness

Nawadon Petchwattana, Phisut Naknaen & Borwon Narupai

To cite this article: Nawadon Petchwattana, Phisut Naknaen & Borwon Narupai (2020) A circular economy use of waste wood sawdust for wood plastic composite production: effect of bio-plasticiser on the toughness, International Journal of Sustainable Engineering, 13:5, 398-410, DOI: [10.1080/19397038.2019.1688422](https://doi.org/10.1080/19397038.2019.1688422)

To link to this article: <https://doi.org/10.1080/19397038.2019.1688422>



Published online: 14 Nov 2019.



Submit your article to this journal [↗](#)



Article views: 1589



View related articles [↗](#)



View Crossmark data [↗](#)



Citing articles: 15 View citing articles [↗](#)



A circular economy use of waste wood sawdust for wood plastic composite production: effect of bio-plasticiser on the toughness

Nawadon Petchwattana^a, Phisut Naknaen^b and Borwon Narupai^c

^aDivision of Polymer Materials Technology, Faculty of Agricultural Product Innovation and Technology, Srinakharinwirot University, Nakhon Nayok, Thailand; ^bDivision of Food Science and Nutrition, Faculty of Agricultural Product Innovation and Technology, Srinakharinwirot University, Nakhon Nayok, Thailand; ^cExpert Centre of Innovative Materials, Thailand Institute of Scientific and Technological Research, Pathumthani, Thailand

ABSTRACT

This research aims to improve the toughness of Poly(lactic acid) (PLA)/wood sawdust (WS) composite by plasticising with tributyrin bio-plasticiser. Experimental results showed the toughness achievement of the plasticised PLA/WS composite, which reflected as the increase of the tensile strain at break and impact resistance. Thermal test indicated that the plasticised composites crystallised earlier than neat PLA and PLA/WS at lower crystallisation temperature (T_c) together with the increased degree of crystallinity (X_c). Thermal degradation test revealed that PLA/WS composite were less stable with the plasticiser incorporation, while the heat distortion temperature (HDT) was found to reduce from more than 85°C, in PLA/WS composite, down to less than 60°C when tributyrin was added at 15 wt%. Dynamic mechanical analysis (DMA) indicated that with increasing the tributyrin plasticiser content, the storage modulus (E') was proportionally decreased. Thermogravimetric analysis (TGA) showed that the plasticised PLA/WS composite decomposed earlier than neat PLA and PLA/WS composite due to the decomposition of low molecular weight compositions. Fourier transform infrared (FT-IR) analysis indicated there was no chemical interaction among the raw materials added. The plasticised composites were found to absorb lower amount of water due to the incorporation of non-polar plasticiser.

ARTICLE HISTORY

Received 8 May 2019
Accepted 29 October 2019

KEYWORDS

Biomass materials; environmental product design; sustainable materials; waste minimisation; remanufacturing; reuse and recycling technologies

1. Introduction

Wood plastic composite (WPC) is widely known and used as a building material for the natural wood substitutions and waste utilisation. Its main compositions composed of the polymer matrix and wood sawdust (WS) or other natural fibres (Petchwattana et al. 2017; Prakash et al. 2018). In recent years, the new European bioeconomy strategy directs to promote the sustainable use of renewable resources such as wood and wood-based products. This aims to convert waste into new products or transform the industrial by-products into high value bio-based products (Sommerhuber, Welling, and Krause 2015; McCormick and Kautto 2013). Thus, WPC production is one of technologies which categorized in the bioeconomy strategy.

Nowadays, WPC is produced from various natural fillers and polymer matrices. However, the commercialised WPCs were mainly produced from the petroleum-based plastics namely; polyethylene (PE), polypropylene (PP) and poly(vinyl chloride) (PVC) (Jeamtrakul et al. 2012; Ghani et al. 2016; Haq and Srivastava 2017). Since the last decade, the production of WPC from biodegradable poly(lactic acid) (PLA) has been proposed by many researchers. However, numerous literatures reported that mixing WS to the brittle-natured PLA made it much more brittle. For some specific applications of PLA/WS composite, such as 3D printing filaments, indoor furniture and wood-based toys, they require PLA/wood composites with good mechanical strength and high impact resistance. Thus, the composite products made from PLA are needed to be toughened. Petchwattana and

Covavisaruch (2014) concluded that adding high rubber WS content made the PLA composites much more brittle. The impact resistance of PLA/rubber WS composite decreased from 21 J·m⁻¹ of neat PLA down to 8 J·m⁻¹, when the rubber WS was incorporated at 30 wt%. Due to the poor interfacial adhesion, the tensile strain at break of PLA/pine WS composites was lower than those of pure PLA for all WS contents (Wang et al. 2011). Moreover, the addition of bamboo cellulose fibre was found to reduce the tensile strength, the strain at break as well as the impact strength of PLA (Lu et al. 2014). Therefore, the study on the toughness improvement of PLA/WS composites is needed.

Numerous literatures have reported the toughness improvement methods of WPC. They included (i) adding the compatibilisers, (ii) toughening of WPC by elastomeric particles and (iii) plasticising with the plasticisers. With ethylene acrylate copolymer (EAC), the impact strength and elongation at break of the PLA/kenaf fibre composite improved with increasing content of EAC. This was the result of the establishment of ductile interface between PLA matrix and kenaf fibre (Mat Taib, Hassan, and Mohd Ishak 2014). Wang et al. (2011) concluded that the epoxy silane or ethylene methyl acrylate glycidyl methacrylate was enhanced the wettability and interfacial adhesions between PLA and wood powder together with the remarkable improvement of the impact resistance and strain at break. The identical behaviour was also observed when poly(ethylene glycol) (PEG) was employed to plasticise PLA/cellulose composite (Halász and Csóka 2013). Petchwattana and

Covavisaruch (2014) toughened PLA/rubber wood powder by adding acrylic core-shell rubber particles (CSR). They indicated that modifying PLA/rubber wood powder with 5 wt% CSR was found to improve both the impact strength and the tensile strain at break simultaneously. For 3D printing application, PLA/wood composite was impact-modified by acrylic processing aid (APA) to obtain the WPC filaments (Petchwattana et al. 2019). Both CSR and APA were found to effectively produce PLA composites without sacrificing the mechanical properties. However, these additives were produced from petrochemicals and left over the microplastic particles after the biodegradation process of PLA and wood powder. Thus, the use of fully biodegradable bio-based impact modifier or plasticiser seems appropriate for the environmental point of view. Although there are many reports on plasticised PLA composites, the mechanical improvements are still limited and the biodegradability issue of the toughening agent added still generated the microplastics.

Maiza et al. (2015) blended two types of bio-based plasticisers, namely triethyl citrate (TEC) and acetyl tributyl citrate (ATBC) to PLA. They found that the plasticised PLA showed the decrements in the storage modulus (E') and thermal stability. Our previous work on studying the effect of bio-based plasticiser molecular weight (MW), glycerol ($MW = 92 \text{ g}\cdot\text{mol}^{-1}$), tributyrin ($MW = 302 \text{ g}\cdot\text{mol}^{-1}$), trilaurin ($MW = 639 \text{ g}\cdot\text{mol}^{-1}$) and tristearin ($MW = 891 \text{ g}\cdot\text{mol}^{-1}$), on the toughness of PLA informed that tributyrin was the most suitable plasticiser of PLA. This was believed that the proper plasticiser molar mass should be ranged from 300 to $400 \text{ g}\cdot\text{mol}^{-1}$ which could be penetrated between PLA chains and lubricate the molecules during deformation process then retarding PLA failure. Experimental results revealed that plasticising PLA with tributyrin was found to increase the tensile strain at break and impact strength by 150% and 26% respectively (Petchwattana, Sanetuntikul, and Narupai 2018a).

To remedy the problem of brittleness as well as maintaining its full biodegradability, this research focuses on the improvement of the toughness of PLA/WS composite by plasticisation technique. Tributyrin was employed as bio-based plasticiser to plasticise PLA composites at 2.5, 5.0, 10 and 15 wt%. To evaluate the plasticisation efficiency and toughness improvement, dynamic mechanical, thermal, chemical as well as morphological properties were tested in neat PLA, PLA/WS and plasticised PLA/WS composites.

2. Materials, processing and testing

2.1. Raw materials

The polymer matrix used in the current research is an extrusion grade PLA (NatureWorks® PLA2003D). It has a molecular weight of $246,500 \text{ g}\cdot\text{mol}^{-1}$ (Paydayesh, Azar, and Arani 2015) with 4% d-lactide and 96% l-lactide (Gonçalves et al. 2018). It has a density, melting point (T_m) and melt flow index (MFI) of $1.24 \text{ g}\cdot\text{cm}^{-3}$, 150.9°C and $6 \text{ g}\cdot 10\text{min}^{-1}$ respectively. WS was received as waste from Mow Heng Li Sawmill in Ayutthaya province, Thailand. It was the mixture of the waste from Burma padauk (*Pterocarpus macrocarpus*), Teak wood (*Tectona grandis*), Iron wood (*Xylia xylocarpa*) and Siamese Sal (*Shorea obtusa*). WS was further prepared by grinding and sieving to the top cut size of $595\mu\text{m}$ (30 mesh). Tributyrin ($\text{C}_{15}\text{H}_{26}\text{O}_6$) is a triglyceride which naturally found in butter. It is composed of butyric acid and glycerol. It was supplied by U&V Holding Co. Ltd. and was added as a plasticiser in this research. It has a molecular weight of $302 \text{ g}\cdot\text{mol}^{-1}$ and a boiling point at 310°C . The chemical structure of tributyrin is clearly presented in Figure 1.

2.2. Plasticisation of PLA/WS by tributyrin

Firstly, PLA was dried in a vacuum oven at 65°C for 12 hr to reduce the hydrolysis and remove moisture. Tributyrin was kept in a desiccator overnight. PLA, WS and tributyrin were dry-blended by a high-speed mixer following the formulation listed in Table 1. Each dry-blended formulation in Table 1 was then melt-mixed by a twin screw extruder (Charoen Tut, CTE-D16L40) and then pelletised to obtain the PLA, PLA/WS and plasticised PLA/WS compound pellets. The set temperature along the extruder barrel was $155/165/180/185/185^\circ\text{C}$ with the screw speed of 80 rpm. The compound pellets were then processed by an injection moulding machine (Charoen Tut, INJ101T) to fabricate the mechanical, thermal, chemical, physical and morphological test specimens.

2.3. Testing and characterisations

To evaluate the strength and toughness of the PLA/WS and plasticised PLA composites, tensile and impact tests were employed to measure the tensile strength, elongation at break and impact strength. The tensile properties were tested at

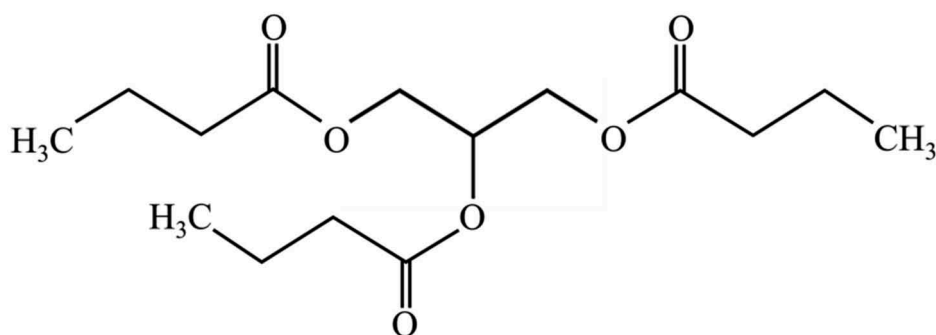


Figure 1. Chemical structure of tributyrin.

Table 1. Blend formulations of PLA, WS and tributyrin.

Formulation code	Raw materials content (wt%)		
	PLA	WS	Tributyrin
PLA	100	-	-
PW	70.0	30	-
PTW2.5	67.5	30	2.5
PTW5	65.0	30	5.0
PTW10	60.0	30	10
PTW15	55.0	30	15

room temperature in accordance with ASTM D638 by an Instron universal testing machine (INSTRON, 5966). The crosshead speed was 5 mm/min, while a gauge length was set at 1 in. The notched Izod impact strength was tested by using an impact tester (ZWICK, BPI-2 5 COM) following ASTM D256. The test specimens were V-notched at 45° for the crack initiation before impact testing. The reported mechanical tests values were the average of 10 replicated samples.

The microscopic observation was performed on the impact fractured surfaces of the neat PLA, PLA/WS and plasticised PLA/WS composites by using a Field Emission Scanning Electron Microscope (FE-SEM) (Hitachi, 4700e) at the accelerating voltage of 1.0–3.0 kV. The test specimen of each formulation was placed on an aluminium stub and coated with a thin layer of gold prior to observation.

A Differential Scanning Calorimeter (DSC) (PerkinElmer, DSC6000) was used to measure the thermal transition of the neat PLA, PLA/WS and plasticised PLA composites. The test conditions composed of five thermal scanning steps as indicated in our previous work. The degree of crystallinity (X_c) is estimated by Equation (1) (Petchwattana, Sanetuntikul, and Narupai 2018a).

$$X_c = 100 \times \frac{\Delta H_M - \Delta H_C}{x_p \times \Delta H^0} \quad (1)$$

where ΔH_m , ΔH_c and x_p are the melting enthalpy, crystallisation enthalpy and weight fraction of PLA in each formulation, respectively. ΔH^0 is the heat of fusion obtained from the melting enthalpy of 100% crystalline PLA, which is 93 J·g⁻¹ (Petchwattana et al. 2018b; Petchwattana and Narupai 2019).

The heat distortion temperature (HDT) test of the plasticised PLA composites was conducted in accordance with ASTM 648 by using a heat distortion tester (GOTECH, HV-3000-P3C) with the applied stress of 1.82 MPa. The measurement was conducted at a heating rate of 2°C·min⁻¹ until the test specimen was deflected at 0.25 mm.

Water absorption test was conducted on neat PLA, PLA/WS and plasticised PLA/WS composites following ASTM D 570. The test was done by measuring the weight change of WPC specimen, which had been soaked in distilled water for 90 days. The water uptake in percentage was calculated following Equation (2) (Petchwattana et al. 2017; Kaboorani 2017).

$$WA(\%) = 100 \times \frac{W_t - W_0}{W_0} \quad (2)$$

where WA is the water absorption in per cent, W_0 is the initial weight and W_t is the weight of the tested specimen at time t , respectively.

Thermogravimetric analysis (TGA) and differential thermal analysis (DTA) were employed to investigate the thermal degradation characteristics and the residual mass of the neat PLA, PLA/WS and plasticised PLA composites by using a thermogravimetric analyser (NETZSCH, STA449F3), under nitrogen atmosphere at a heating rate of 10°C·min⁻¹.

A Fourier transform infrared spectroscopy (FT-IR) (Nicolet, iS 5) was employed to observe the chemical interaction between PLA, WS and tributyrin. Each sample was scanned at wavenumber of 650–4000 cm⁻¹.

The melt flow index (MFI) was observed following the method described in ASTM D 1238 by a melt flow indexer (Charoen Tut, MFI01T). The temperature and the piston load were 210°C and 2.16 kg, respectively.

Dynamic mechanical analysis (DMA) of neat PLA, PLA/WS composites with and without tributyrin was carried out by a Mettler Toledo dynamic mechanical analyser. The test was conducted with a tension mode from 0 to 150°C at a heating rate, frequency and amplitude of 2°C·min⁻¹, 1 Hz and 10.00 μm, respectively.

3. Results and discussions

3.1. Morphological and mechanical studies

Figure 2 illustrates the FE-SEM micrograph of the neat PLA, PLA/WS composite and PLA/WS composite with tributyrin. Neat PLA was fractured with smooth surface, which indicated that the crack was propagated rapidly during the impact fracture process. With the addition of WS, some pulled-out WS particles were observed together with the interfacial voids between PLA matrix and WS particles. Moreover, the smooth PLA matrix surface and the clear boundary between the two materials were presented, which correlated to the non-wettability between PLA and WS particles (Lv et al. 2015). This confirmed the poor interphase bonding and incompatibility between two different materials. With 10 and 15 wt% tributyrin (Figure 2(c,d)), rougher fracture surfaces were observed in the PLA matrix, while the poor interfacial adhesion was still evidenced. Some pulled-out WS particles and the interfacial boundary between PLA and WS was still observed. In this case, the energy required to fracture the specimen was increased, due to the plasticised PLA matrix, but the poor polymer matrix-filler stress transfer still existed. Figure 3 shows the fracture surfaces of PLA matrix at higher magnification. Neat PLA and PLA/WS composite exhibited very smooth fracture surfaces and allowed the crack to propagate easily under impact force. Plasticising PLA/WS composite with 15 wt% tributyrin was found to induce the rougher fracture surface together with the localised plastic deformations (Figure 3(c,d)). This required much more energy to rupture the test specimen and significantly improved the impact strength of the composites.

As shown in Table 2, the tensile strength, tensile elongation at break and impact resistance were all dropped when WS was added to PLA due to the bad interfacial bonding and the brittle nature of PLA. These limited the PLA-WS stress transfer and restricted the PLA chain entanglement during tensile test as previously discussed in Figures 2–3. Plasticising PLA/WS

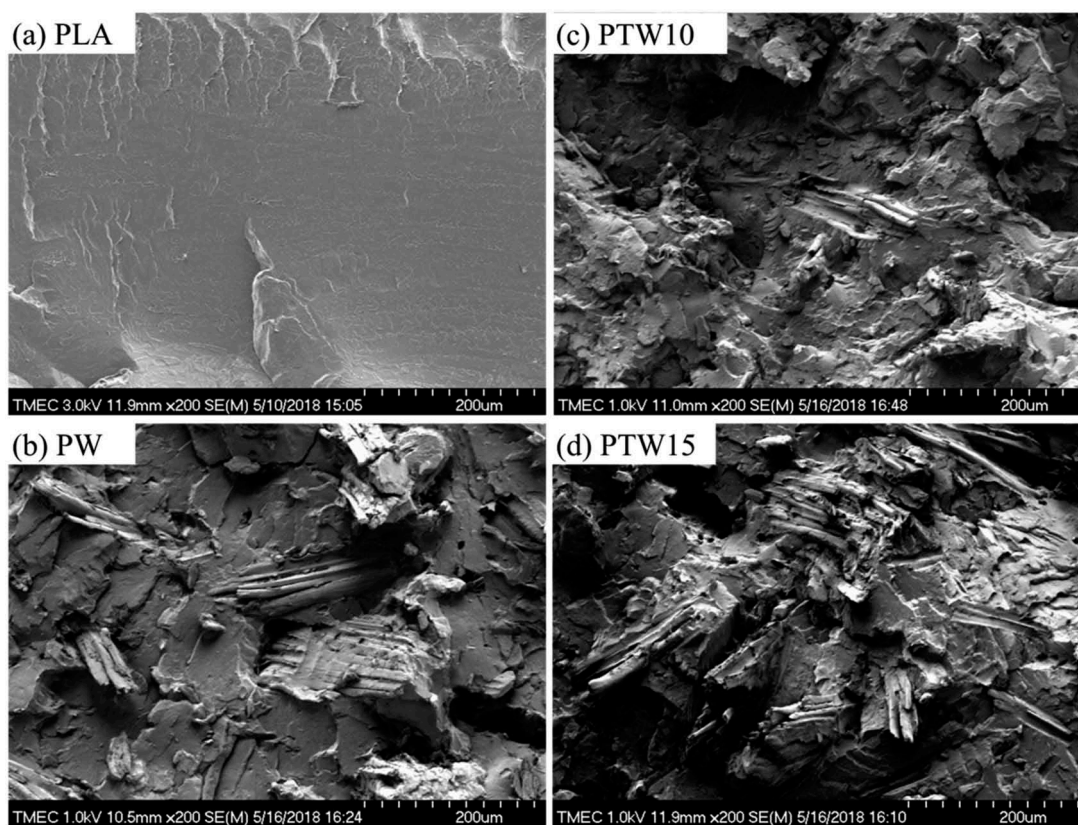


Figure 2. FE-SEM micrograph of neat PLA, PLA/WS and plasticised PLA/WS composites.

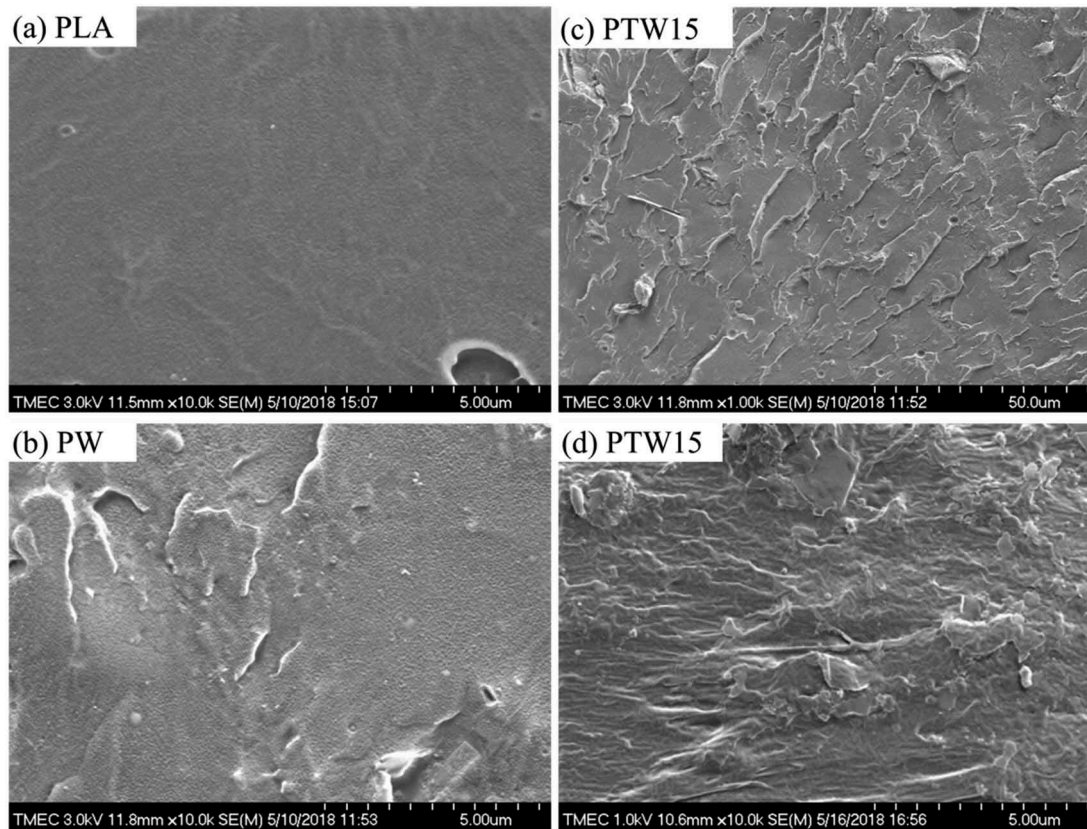


Figure 3. Highly magnified FE-SEM micrograph of neat PLA, PLA/WS and plasticised PLA/WS composites.

Table 2. Mechanical properties and MFI of PLA, PLA/WS and plasticised PLA/WS composites.

Formulation code	Tensile strength (MPa)	Elongation at break (%)	Impact strength ($\text{J}\cdot\text{m}^{-1}$)	MFI at 210°C ($\text{g}\cdot 10\text{ min}^{-1}$)
PLA	66.4 \pm 3.65	3.08 \pm 0.45	26.7 \pm 1.42	7.8
PW	40.5 \pm 2.12	2.53 \pm 0.61	23.2 \pm 1.20	6.2
PTW2.5	33.6 \pm 2.01	4.93 \pm 1.63	25.6 \pm 2.64	6.9
PTW5	29.7 \pm 2.05	7.01 \pm 2.68	29.3 \pm 1.50	7.4
PTW10	16.6 \pm 2.27	23.5 \pm 3.60	37.8 \pm 1.24	7.6
PTW15	14.3 \pm 1.84	25.8 \pm 6.91	39.1 \pm 2.75	8.0

composite with tributyrin (PTW2.5, PTW5, PTW10 and PWT15) was further decreased the tensile strength due to the plasticisation effect as previously observed in other plasticised PLA systems (Courgneau et al. 2011; Carbonell-Verdu et al. 2017; Petchwattana, Sanetuntikul, and Narupai 2018a). The tensile strength reduced from 40.5 MPa, in PLA/WS composite, down to 33.6, 29.7, 16.6 and 14.3 MPa for 2.5, 5.0, 10 and 15 wt % tributyrin, respectively. The plasticised PLA/WS composite are the result of softening effect derived from the softened PLA matrix and PLA chain lubrication. This behaviour is in agreement with the previous reports on the plasticised WPC systems. Plasticising PLA/microcellulose composite with 10 wt% poly (ethylene glycol) (PEG) was reported to reduce the tensile strength by more than two times (Murariu et al. 2008a; Halász and Csóka 2013). With the addition of triacetin, the tensile strength of PLA/kenaf blast fibre composite reduced with increasing triacetin loading (Ibrahim et al. 2010).

The toughness of polymer or polymer composites is generally evaluated by the tensile elongation at break and impact strength (Murariu et al. 2008b). As shown in Table 2, the tensile strain at break and the impact strength of PLA significantly reduced with the addition of WS, due to the restriction of PLA chain entanglement and the poor interfacial bonding between two raw materials. Adding tributyrin to PLA/WS composite gradually improved the elongation at break from 2.53% in PLA/WS to 25.8% in PLA/WS/15 wt% tributyrin. This phenomenon was mainly due to the PLA chain lubrication during the applied tensile load which facilitated the chain entanglement (Graupner et al. 2016; Petchwattana et al. 2019). For the impact strength, it increased from 23.2 to 39.1 $\text{J}\cdot\text{m}^{-1}$ for the PLA composite with 15 wt% tributyrin. This was mainly due to the plastic deformation, which required much more energy to fracture the specimen as observed by FE-SEM. Literature reviews indicated that PLA was more brittle with the addition of lignin. For the ternary blend of PLA/lignin/PEG, it exhibited higher deformability compared with those of the unplasticised PLA/lignin composites (Rahman et al. 2013). Epoxidised linseed oil (ELO) was found to provide the plasticisation effect in PLA/hazelnut shell flour (HSF) composites. Both the tensile strength reduced with increasing ELO content, while the elongation at break increased. However, adding ELO by more than 15 wt% led to the phase separation (Balart et al. 2016). Chieng et al. (2014) further summarised that at high plasticiser concentrations, a small part of them was directly in contact with the interfacial area of the composites and the excess amount was scattered in the polymeric matrix. This was the cause of the tensile strength reduction. The increase in the tensile elongation at break was mainly due to the

reduction of the intermolecular force between PLA chains and the chain mobility improvement induced by plasticiser (Balart et al. 2016; Burgos, Martino, and Jimenez 2013).

3.2. Melt flow index (MFI)

The MFI values (in Table 2), determined at 210°C, showed that adding WS to PLA decreased the MFI due to the PLA molecular mobility restriction and the composite fluidity reduction induced by the WS particles. With the presence of tributyrin, the MFI was found to increase by around 1–2 $\text{g}\cdot 10\text{ min}^{-1}$ due to the molecular lubrication facilitated by tributyrin. Numerous literatures indicated that both MFI and melt volume rate (MVR) of the plasticised PLA composites increased with the acetyl tributyl citrate loading (Scatto et al. 2013) and epoxidised soybean oil (ESO) (Xu and Qu 2009) plasticisers.

3.3. DSC measurements

Thermal transition temperatures obtained from DSC thermogram in Figure 4, their area under peaks and the estimated X_c are clearly indicated in Table 3. Neat PLA showed the glass transition temperature (T_g) at around 62°C and it slightly reduced with the addition of WS by around 1°C. With the addition of tributyrin, the T_g gradually dropped by around 2°C to 11°C. This was due to the segmental mobility enhancement induced by the tributyrin plasticiser (Chieng et al. 2014). The crystallisation temperature (T_c) of PLA composite was found to significantly reduce in parallel with that of T_g from 121.2°C, in PLA/WS composite, to 101.1°C in PLA/WS composite with 15 wt% plasticiser. This indicated the good compatibility between PLA and tributyrin (Chieng et al. 2013). The melting temperature (T_m) of the PLA and PLA/WS composite showed single melting endotherm, while the plasticised PLA/WS composite exhibited double melting peaks since tributyrin was added at least 10 wt% due to the melt of different crystal structures (Petchwattana et al. 2018b). The T_m was found to vary in a small gap by around 1°C, while the area under T_m peaks slightly increased with the plasticiser added. Compared to those of neat PLA and PLA/WS composite, the plasticised PLA exhibited higher X_c due to the increase of PLA chain mobility which accelerated the crystallisation rate of the composites. This allowed the plasticised PLA composites to crystallise earlier at lower T_c with higher crystalline region (Kulinski and Piorkowska 2005; Chieng et al. 2013).

3.4. Dynamic mechanical properties

Figure 5 illustrates the storage modulus (E') and $\tan \delta$, as a function of temperature, of the neat PLA, PLA/WS composites with and without tributyrin plasticiser. Technically, the drop of E' value represents the glass transition (T_g) and the immediate increases of E' after T_g is normally known as the cold crystallisation temperature (T_{cc}) (Petchwattana, Sanetuntikul, and Narupai 2018a). In Figure 5(a), neat PLA showed T_g at around 76.39°C. With the addition of WS, the T_g reduced by around 18°C while the E' value dropped significantly. The

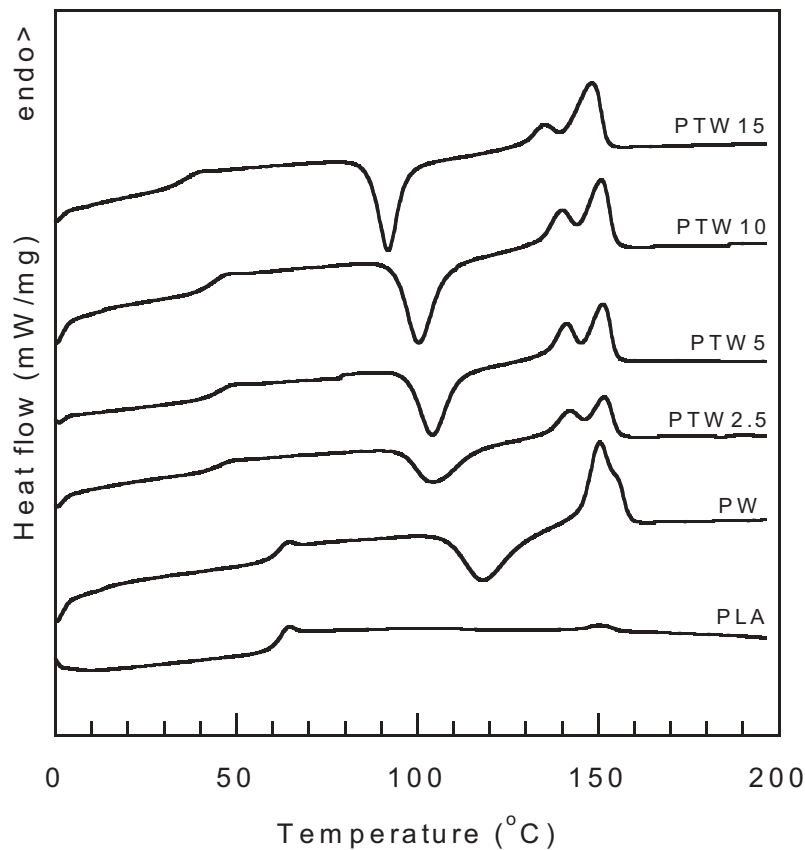


Figure 4. DSC second heating scan of neat PLA, PLA/WS and plasticised PLA/WS composites.

Table 3. Thermal properties of PLA, PLA/WS and plasticised PLA/WS composites.

Formulation code	T_g (°C)	T_c (°C)	ΔH_c (J·g ⁻¹)	T_{m1} (°C)	T_{m2} (°C)	ΔH_m (J·g ⁻¹)	X_c (%)
PLA	62.19	123.8	18.28	-	150.9	19.23	1.02
PW	61.53	118.2	19.85	-	152.9	21.86	3.09
PTW2.5	45.87	104.6	18.62	141.5	152.3	21.46	4.52
PTW5	45.20	104.5	17.76	141.3	151.6	20.10	3.87
PTW10	43.04	100.6	20.52	141.0	152.1	23.91	6.08
PTW15	36.38	91.16	22.64	135.5	149.2	25.64	5.87

reduction of E' was mainly due to the lack of stress transfer from the PLA matrix to WS particles (Petchwattana and Covavisaruch 2014; Petchwattana, Sanetuntikul, and Narupai 2018a) as evidenced by FE-SEM in Figure 2. Further T_g and E' reductions were clearly found when tributyrin was added to PLA/WS composite. With increasing plasticiser content from 0 to 2.5, 5, 10 and 15 wt%, both the E' and T_g values were proportionally decreased. The minimum T_g , at 37.80°C, was found when tributyrin plasticiser was added at 15 wt%. This shift was mainly due to the mobility increment of amorphous phases of PLA chains derived by plasticiser (Teymoorzadeh and Rodrigue 2015; Petchwattana, Sanetuntikul, and Narupai 2018a; Satapathy and Kothapalli 2018)

Tan δ is widely known as the ratio of the loss modulus (E'') to the storage modulus (E') which measures the loss of energy in relation to the recoverable energy. The peak of tan δ correlates to the α -relaxation processes and T_g of polymers (Teymoorzadeh and Rodrigue 2015; Petchwattana, Sanetuntikul, and Narupai 2018a; Satapathy and Kothapalli 2018). As shown in Figure 5(b),

both the tan δ peak position and height were varied due to the addition of tributyrin as previously observed in E' . In neat PLA, a single peak was observed at 64.70°C. With the incorporation of tributyrin, the tan δ peak was shifted to the lower position at 62.31°C, 54.97°C, 54.73°C and 41.95°C for the composites with 2.5, 5, 10, 15 and 20 wt% tributyrin respectively. Moreover, the tan δ peak height value decreased from 2.86, in neat PLA, down to 0.560 when tributyrin was added at 15 wt%. The plasticisation effect was believed to smoothen the PLA chain and facilitate the chain mobility by decreasing the internal friction (Teymoorzadeh and Rodrigue 2015; Petchwattana, Sanetuntikul, and Narupai 2018a; Satapathy and Kothapalli 2018).

3.5. Heat distortion temperature (HDT)

HDT is one of the significant parameters indicating the service temperature of polymers as well as polymer composites. Figure 6 shows the HDT value for neat PLA, PLA/WS and plasticised PLA/WS composites. The HDT value of neat PLA was less than 60°C. With the addition of WS, the HDT value of the composite increased to more than 85°C. However, it gradually decreased with the tributyrin content down to less than 60°C when tributyrin was added at 15 wt%. This behaviour was expected and generally observed in other plasticised PLA systems. The HDT of PLA composite significantly reduced with the ELO from around 54.5°C to less than 50°C (Balart et al. 2016). Plasticising PLA with octyl epoxy stearate (OES)

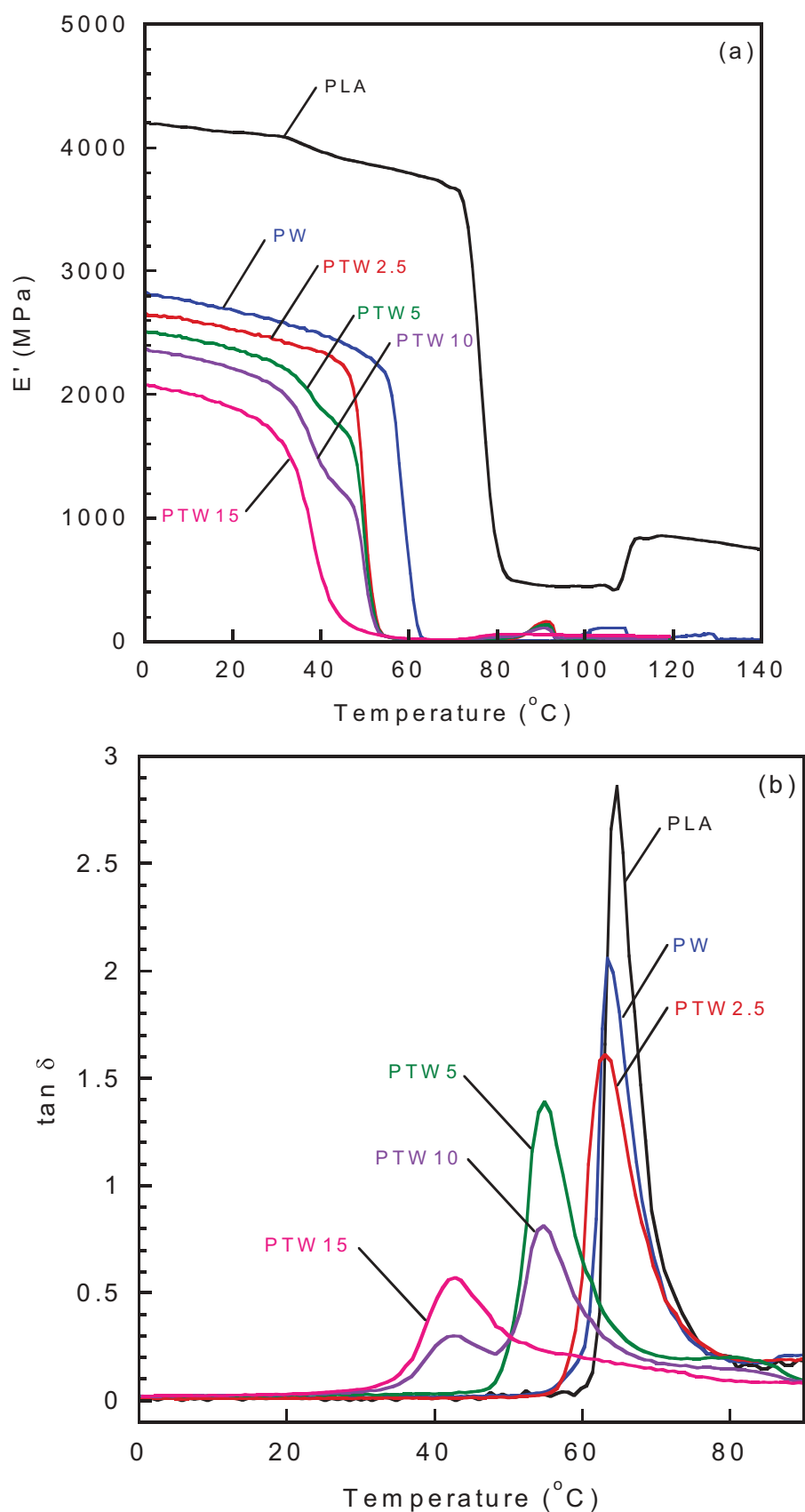


Figure 5. Dynamic mechanical properties of neat PLA, PLA/WS and plasticised PLA/WS composites: (a) storage modulus and (b) $\tan \delta$.

reduced the HDT of PLA from 47.6 $^{\circ}\text{C}$ to 46.6 $^{\circ}\text{C}$ (Ferri et al. 2016a). With maleinised linseed oil (MLO) the HDT of PLA

composite was also dropped from 49.9 $^{\circ}\text{C}$ down to 44.8 $^{\circ}\text{C}$ (Ferri et al. 2016b).

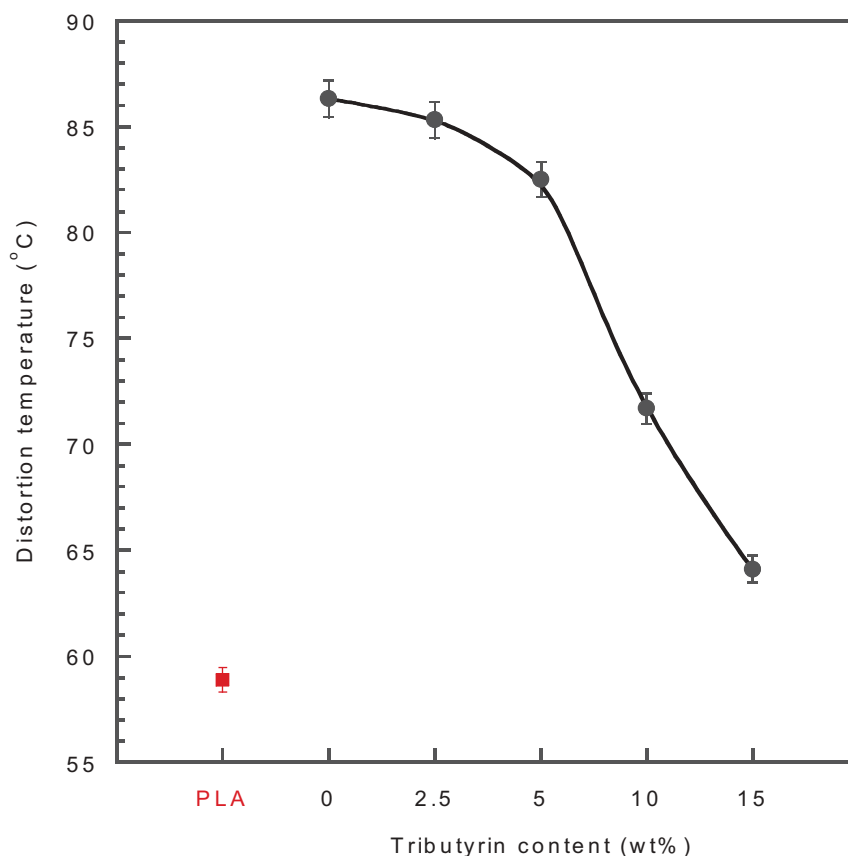


Figure 6. Heat distortion temperatures of neat PLA, PLA/WS and plasticised PLA/WS composites.

3.6. Degradation temperature

Figure 7 shows the thermogravimetric (TG) and DTA thermograms of PLA, PLA/WS and plasticised PLA composites. Their estimated T_{d10} , T_{d50} and residual mass are clearly listed in Table 4. In Figure 7(a), the decomposition curve characteristic of PLA/WS composite was similar to those of neat PLA and PLA/WS composite and it occurred over a single step. Neat PLA started to decompose at around 310°C and it continued decomposing until 390°C with the residual mass of 1.16%. With the addition of WS, the composite decomposed earlier at the temperature of 250°C. This was a result of the decomposition of low molecular weight hemicellulose and extractives. The T_{d10} , T_{d50} and residual mass were 327°C, 354°C and 10%, respectively. The plasticised PLA composites decomposed more than two steps. The first one was the decomposition of hemicellulose followed by the decompositions of cellulose, tributyrin, PLA and lignin (Tajvidi and Takemura 2010). This reduced the onset temperature below 200°C together with the reduced T_{d10} and T_{d50} , indicating that there was no chemical bonding between PLA, WS and tributyrin. The DTG curves in Figure 7(b) provide better understanding of the thermal degradation behaviour of PLA/WS composite with various tributyrin contents. Neat PLA showed a single decomposition stage corresponding to that observed in TG result. With the additions of WS and tributyrin, the composites started to decompose earlier than neat PLA at a temperature range of 250–300°C corresponding to the decomposition of hemicellulose which is the least thermally stable lignocellulosic composition in WS (Tajvidi and Takemura 2010). The

second decomposition occurred at 300–400°C related to the decomposition of cellulose, tributyrin and PLA. In comparison, the addition of tributyrin reduced the T_d for all concentrations. This is mainly due to (i) the tiny molecules of tributyrin which requires less energy to decompose and (ii) the hydrolysis of PLA molecules during the melt blending with WS and injection process. These results are in accordance with the PLA/kenaf fibre composite plasticised with triacetin, where its degradation temperature was less than neat PLA (Ibrahim et al. 2010). However, the increased thermal stability of the plasticised PLA composites was found only for the system with the intermolecular bonding between PLA, WS and plasticiser. The decomposition temperature of the PLA composite plasticised with epoxidised palm oil (EPO) significantly increased by more than 30°C with increasing EPO concentration. Further investigation by FT-IR spectroscopy indicated the chemical interaction between the epoxy group of EPO and the hydroxyl group of PLA (Chieng et al. 2014). This enlarged the PLA molecules and required more energy to decompose. The identical behaviour was also found in the PLA composites with ELO (Balart et al. 2016) and ESO (Blend et al. 2012).

3.7. FT-IR analysis

Figure 8 illustrates the infrared spectra for the neat PLA, PLA/WS and plasticised PLA/WS composites. For all samples tested, they show the identical peak characteristics which related to their parent materials. The peaks at 1748 cm^{-1} and 1184 cm^{-1} indicate the C=O stretching and C–O–C stretching of PLA. The large and

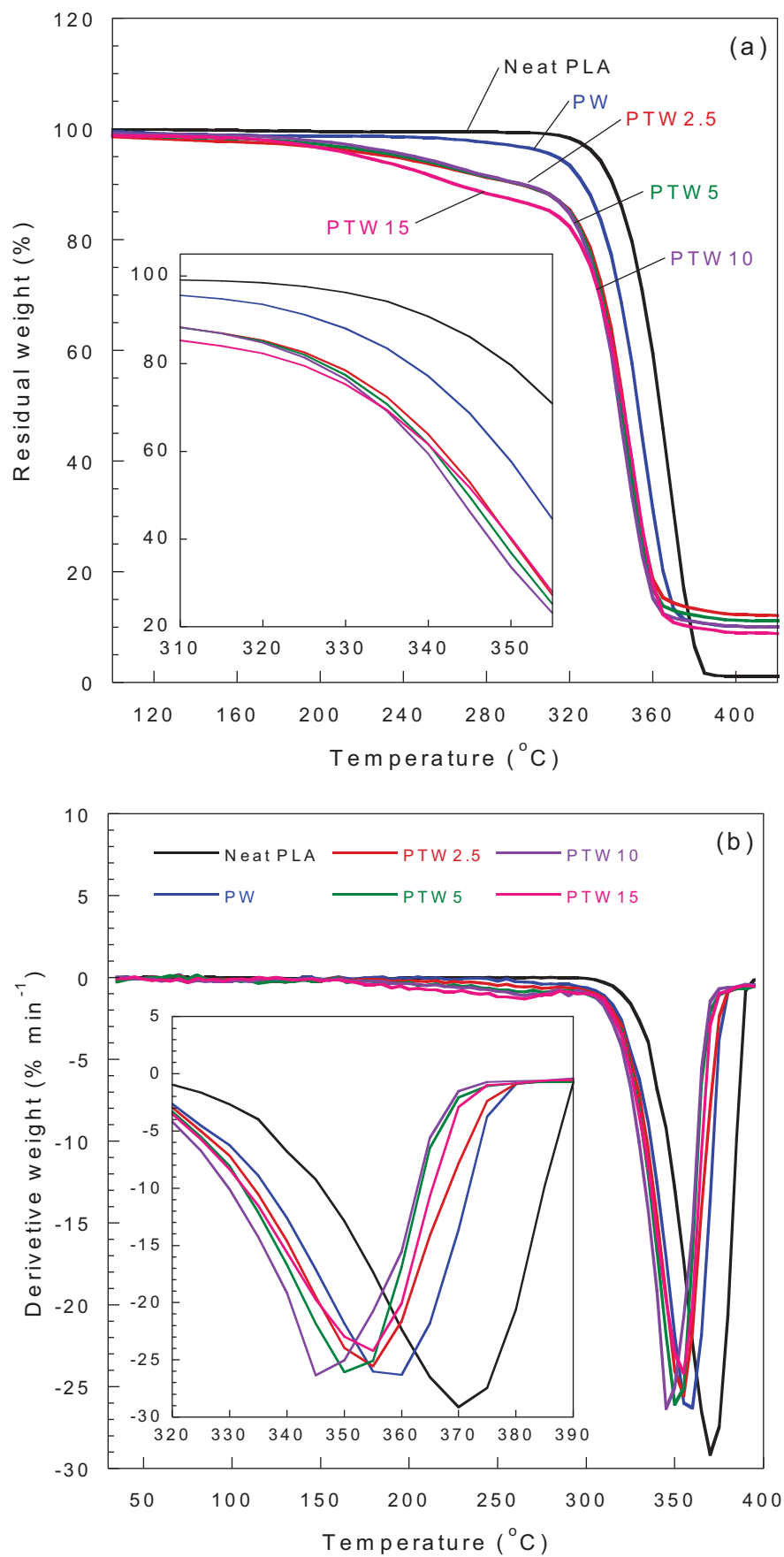


Figure 7. TG/DTG thermogram of neat PLA, PLA/WS and plasticised PLA/WS composites: (a) TG and (b) DTG.

Table 4. Thermal degradation of PLA, PLA/WS and plasticised PLA/WS composites.

Formulation code	T _{onset} (°C)	T _{d10} (°C)	T _{d50} (°C)	Residual mass (%)
PLA	310	340	363	1.16
PW	250	327	354	10.0
PTW2.5	193	295	346	12.1
PTW5	192	295	345	11.1
PTW10	190	294	344	10.0
PTW15	185	269	344	8.86

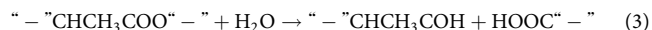
T_{d10} = 10% weight loss temperatureT_{d50} = 50% weight loss temperature

broad spectra at 3500–3000 cm⁻¹ and a small peak at 2942 cm⁻¹ are the O–H stretching. With the presence of WS, these O–H groups are still found at the same position, which indicated there was no chemical interaction between PLA and WS. Moreover, there were no changes in chemical composition and peak shifts in the plasticised PLA/WS samples. This could be summarised that there was no chemical interaction among the raw materials added in the composites. Maizatul et al. (2013) indicated that there was no chemical linkage between the triacetin-plasticised PLA/kenaf bast fibre (KBF) composites. With further alkali treatment, the FT-IR peaks characteristic were still unchanged. However, Mofokeng et al. (2011) found the hydrogen bonding between PLA/sisal fibre composites with the annealing process.

3.8. Water absorption

Figure 9 shows the water uptake of the neat PLA, PLA/WS and plasticised PLA composites after the specimens had been soaked in the distilled water for 90 days. Neat PLA absorbed water by around 1% due to its hydrophobicity. With the presence of WS, the water absorption dramatically increased by nearly 8%, due to the addition of the hydrophilic part and the

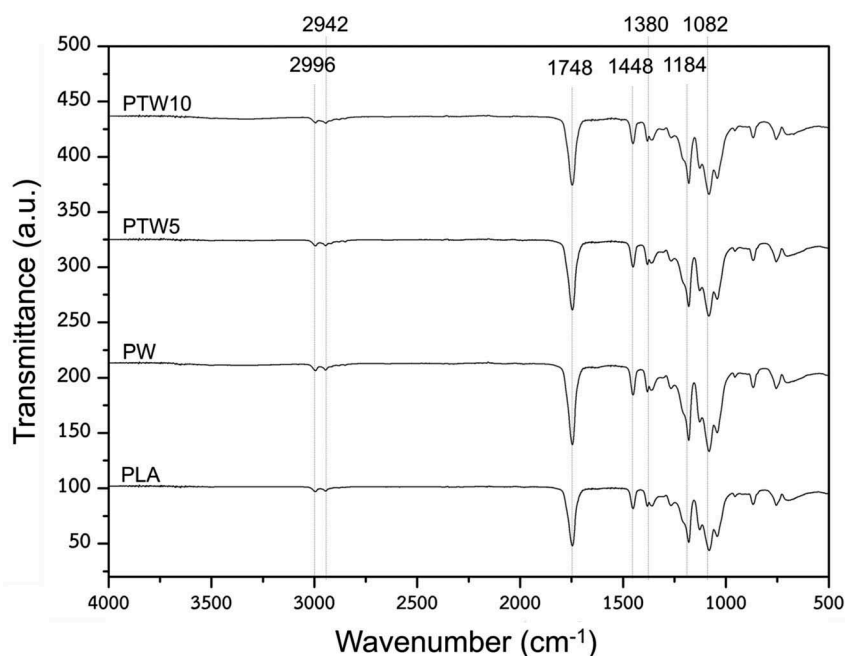
occurrence of some interfacial voids between PLA and WS as discussed in Figure 2. For the plasticised PLA/WS composite, the water uptake significantly reduced due to the incorporation of non-polar plasticiser. This plasticiser was penetrated through the WS particles, interfacial voids as well as free volume in PLA matrix and possibly prevented the diffusion of water molecules (Petchwattana and Sanetuntikul 2018; Petchwattana et al. 2019). During water absorption process, the hydrolysis reaction of PLA was possible taken place as follows :



Under water absorption test, the –CHCH₃COO– groups in PLA reacted with water molecules which generated the low molecular weight substances and cut the PLA chains (David and Yang 2006). Ahmad-Faris, Haruo, and Yoshihito (2008) found the reduction of PLA molecular weight under the hydrolytic condition. This reaction was strongly depended on the time and temperature.

4. Conclusions

In this research, the PLA/WS composite was plasticised with different concentrations of tributyrin from 2.5 to 15 wt%. Mechanical test results showed that the plasticisation effect brought PLA composites less stiff and tougher, which reflected as the reduced tensile strength, the increased elongation at break and impact strength. FE-SEM revealed the poor interphase bonding between PLA and WS particles together with the smooth fracture surface. However, the addition of tributyrin to the PLA composite made the fracture surface rougher and the localised plastic deformation was observed. Thus, the main goal of the toughness improvement of the PLA/WS composite was

**Figure 8.** FT-IR spectra of neat PLA, PLA/WS and plasticised PLA/WS composites.

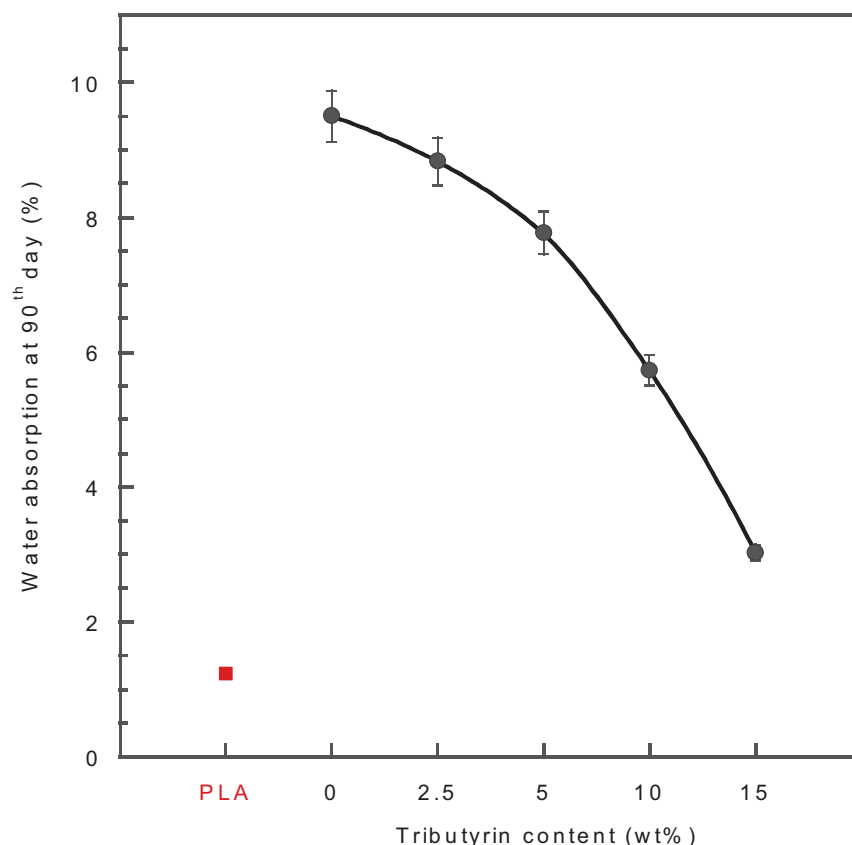


Figure 9. Water uptake of neat PLA, PLA/WS and plasticised PLA/WS composites at ninetyth day immersion.

achieved. Thermal test results indicated that the plasticised composites crystallise at lower temperature with higher degree of crystallinity. TG/DTA results showed that the plasticised PLA/WS composite decomposed earlier than neat PLA and PLA/WS composites due to the decomposition of low molecular weight compositions. FT-IR analysis indicated that there was no chemical linkage among the raw materials added. With increasing the plasticiser content from 0 to 2.5, 5, 10 and 15 wt%, both the E' and T_g values, obtained from DMA, were proportionally decreased. The plasticised composites were found to absorb lower amount of water due to the incorporation of non-polar phase.

Acknowledgements

The authors would like to thank Srinakharinwirot University for financial support (Contract no. 029/2560). Thanks are expanded to Mr. Kittisak Phromsuk, Miss. Suphaphon Phetsamai and Miss. Pikul Sukplang for their assistance.

Disclosure statement

No potential conflict of interest was reported by the authors.

Funding

This work was supported by the Srinakharinwirot University [029/2560].

Notes on contributors

Nawadon Petchwattana was born in Bangkok in 1983. He is an Associate Professor in Polymer Science at Srinakharinwirot University and a member of the B.Sc. in Polymer Innovation and Management programme. His areas of interest and research are in the waste utilisations, biodegradable polymers and antimicrobial packaging.

Phisut Naknaen was born in Phuket in 1984. He is an Assistant Professor in Food Technology at Srinakharinwirot University and member of the B. Sc. in Food Science and Nutrition programme. His areas of interest and research are in the food waste utilisations, food chemistry and low energy food products.

Borwon Narupai is a researcher in the Expert Centre of Innovative Materials, Thailand Institute of Scientific and Technological Research (TISTR). His areas of interest and research are in the rubber products development, bio-based and biodegradable materials.

ORCID

Nawadon Petchwattana  <http://orcid.org/0000-0001-6713-8547>

Phisut Naknaen  <http://orcid.org/0000-0002-0091-7025>

References

- Ahmad-Faris, M. A., N. Haruo, and S. Yoshihito. 2008. "Evaluation of Kinetics Parameters for poly(l-lactic acid) Hydrolysis under High-pressure Steam." *Polymer Degradation and Stability* 93: 1053–1058. doi:10.1016/j.polymdegradstab.2008.03.022.
- Alavudeen, A., N. Rajini, S. Karthikeyan, M. Thiruchitrabalam, and N. Venkateshwareen. 2014. "Mechanical Properties of banana/kenaf Fibre-

- reinforced Hybrid Polyester Composites: Effect of Woven Fabric and Random Orientation." *Materials & Design* 66: 246–257. doi:10.1016/j.matdes.2014.10.067.
- Balart, J. F., V. Fombuena, O. Fenollar, T. Boronat, and L. Sanchez-Nacher. 2016. "Processing and Characterization of High Environmental Efficiency Composites Based on PLA and Hazelnut Shell Flour (HSF) with Biobased Plasticisers Derived from Epoxidised Linseed Oil (ELO)." *Composites Part B: Engineering* 86: 168–177. doi:10.1016/j.compositesb.2015.09.063.
- Blend, V. S., G. Silverajah, N. A. Ibrahim, N. Zainuddin, W. M. Z. W. Yunus, and H. A. Hassan. 2012. "Mechanical, Thermal and Morphological Properties of poly(lactic acid)/epoxidised Palm Olein Blend." *Molecules* 17: 11729–11747. doi:10.3390/molecules171011729.
- Burgos, N., V. P. Martino, and A. Jimenez. 2013. "Characterization and Ageing Study of poly(Lactic Acid) Films Plasticized with Oligomeric Lactic Acid." *Polymer Degradation and Stability* 98: 651–658. doi:10.1016/j.polymdegradstab.2012.11.009.
- Carbonell-Verdu, A., M. D. Samper, D. Garcia-Garcia, L. Sanchez-Nache, and B. Rafael. 2017. "Plasticisation Effect of Epoxidised Cottonseed Oil (ECISO) on poly(lactic acid)." *Industrial Crops and Products* 104: 278–286. doi:10.1016/j.indcrop.2017.04.050.
- Chiang, B. W., N. A. Ibrahim, Y. Y. Then, and Y. Y. Loo. 2014. "Epoxidised Vegetable Oils Plasticized poly(lactic acid) Biocomposites: Mechanical, Thermal and Morphology Properties." *Molecules* 19: 16024–16038. doi:10.3390/molecules191016024.
- Chiang, B. W., N. A. Ibrahim, W. M. Z. W. Yunus, and M. Z. Hussein. 2013. "Plasticized poly(lactic acid) with Low Molecular Weight poly(ethylene glycol): Mechanical, Thermal, and Morphology Properties." *Journal of Applied Polymer Science* 130: 4576–4580.
- Courgneau, C., S. Domenek, A. Guinault, L. Avérous, and V. Ducruet. 2011. "Analysis of the Structure-properties Relationships of Different Multiphase Systems Based on Plasticized poly(lactic acid)." *Journal of Polymers and the Environment* 19: 362–371. doi:10.1007/s10924-011-0285-5.
- David, K., and Y. Q. Yang. 2006. "Molecular Modeling Study of the Resistance of PLA to Hydrolysis Based on the Blending of PLLA and PDLA." *Polymer* 47: 4845–4850. doi:10.1016/j.polymer.2006.05.002.
- Ferri, J. M., D. Garcia-Garcia, L. Sánchez-Nacher, O. Fenollar, and R. Balart. 2016b. "The Effect of Maleinized Linseed Oil (MLO) on Mechanical Performance of poly(lactic acid)-thermoplastic Starch (PLA-TPS) Blends." *Carbohydrate Polymers* 147: 60–68. doi:10.1016/j.carbpol.2016.03.082.
- Ferri, J. M., M. D. Samper, D. Garcia-Sanoguera, M. J. Reig, O. Fenollar, and R. Balart. 2016a. "Plasticising Effect of Biobased Epoxidised Fatty Acid Esters on Mechanical and Thermal Properties of poly(lactic acid)." *Journal of Materials Science* 51: 5356–5366. doi:10.1007/s10853-016-9838-2.
- Ghani, S. A., M. H. M. Pital, F. Zainuddin, and H. Ismail. 2016. "The Effect of the Chemical Modification of Wood Fibre Using Salicylic Acid and Ethanol on the Properties of Recycled High Density polyethylene/wood Fibre Composites." *Journal of Physical Science* 27: 1–14.
- Gonçalves, C., A. Pinto, A. V. Machado, J. Moreira, I. C. Gonçalves, and F. Magalhães. 2018. "Biocompatible Reinforcement of poly(lactic acid) with Graphene Nanoplatelets." *Polymer Composites* 39: E308–E320. doi:10.1002/pc.v39.S1.
- Graupner, N., K. Albrecht, G. Ziegmann, H. Enzler, and J. Müssig. 2016. "Influence of Reprocessing on Fibre Length Distribution, Tensile Strength and Impact Strength of Injection Moulded Cellulose Fibre-reinforced Polylactide (PLA) Composites." *Express Polymer Letters* 10: 647–663. doi:10.3144/expresspolymlett.2016.59.
- Halász, K., and L. Csóka. 2013. "Plasticized Biodegradable poly(lactic acid) Based Composites Containing Cellulose in Micro- and Nanosize." *Journal of Engineering* 2013: 329379. doi:10.1155/2013/329379.
- Hag, S., and R. Srivastava. 2017. "Wood Polypropylene (PP) Composites Manufactured by Mango Wood Waste with Virgin or Recycled PP: Mechanical, Morphology, Melt Flow Index and Crystalline Behavior." *Journal of Polymers and the Environment* 25: 640–648. doi:10.1007/s10924-016-0845-9.
- Ibrahim, N. A., W. M. Z. W. Yunus, M. Othman, K. Abdan, and K. A. Hadithon. 2010. "poly(lactic acid) (Pla)-reinforced Kenaf Bast Fibre Composites: The Effect of Triacetin." *Journal of Reinforced Plastics and Composites* 29: 1099–1111. doi:10.1177/0731684409344651.
- Jeamtrakull, S., A. Kositchaiyong, T. Markpin, V. Rosarpitak, and N. Sombatsompop. 2012. "Effects of Wood Constituents and Content, and Glass Fibre Reinforcement on Wear Behavior of Wood/PVC Composites." *Composites Part B: Engineering* 43: 2721–2729. doi:10.1016/j.compositesb.2012.04.031.
- Kaboorani, A. 2017. "Characterizing Water Sorption and Diffusion Properties of wood/plastic Composites as a Function of Formulation Design." *Construction and Building Materials* 136: 164–172. doi:10.1016/j.conbuildmat.2016.12.120.
- Kulinski, Z., and E. Piorkowska. 2005. "Crystallisation, Structure and Properties of Plasticized poly(L-lactide)." *Polymer* 46: 10290–10300. doi:10.1016/j.polymer.2005.07.101.
- Lu, T., S. Liu, M. Jiang, X. Xu, Y. Wang, Y. Wang, J. Gou, D. Hui, and Z. Zhou. 2014. "Effects of Modifications of Bamboo Cellulose Fibres on the Improved Mechanical Properties of Cellulose Reinforced poly(lactic acid) Composites." *Composites Part B: Engineering* 62: 191–197. doi:10.1016/j.compositesb.2014.02.030.
- Ly, S., H. Tan, J. Gu, and Y. Zhang. 2015. "Silane Modified Wood Flour Blended with poly(lactic acid) and Its Effects on Composite Performance." *BioResources* 10: 5426–5439. doi:10.15376/biores.10.3.5426-5439.
- Maiza, M., M. T. Benaniba, G. Quintard, and V. Massardier-Nageotte. 2015. "Biobased Additive Plasticising Poly(lactic acid) (PLA)." *Polímeros* 25: 581–590. doi:10.1590/0104-1428.1986.
- Maizatun, N., I. Norazowa, W. M. Z. W. Yunus, A. Khalina, and K. Khalisanni. 2013. "FTIR and TGA Analysis of Biodegradable poly(lactic acid)/treated Kenaf Bast Fibre: Effect of Plasticisers." *Pertanika Journal of Science and Technology* 21: 151–160.
- Mat Taib, R., H. M. Hassan, and Z. A. Mohd Ishak. 2014. "Mechanical and Morphological Properties of Poly(lactic acid)/kenaf Bast Fibre Composites Toughened with an Impact Modifier." *Polymer-Plastics Technology and Engineering* 53: 199–206. doi:10.1080/03602559.2013.843709.
- McCormick, K., and N. Kautto. 2013. "The Bioeconomy in Europe: An Overview." *Sustainability* 5: 2589–2608.
- Mofokeng, J. P., A. S. Luyt, T. Tabi, and J. Kovacs. 2011. "Comparison of Injection Moulded, Natural Fibre-reinforced Composites with PP and PLA as Matrices." *Journal of Thermoplastic Composite Materials* 25: 927–948. doi:10.1177/0892705711423291.
- Murariu, M., A. D. S. Ferreira, M. Alexandre, and P. Dubois. 2008a. "Polylactide (PLA) Designed with Desired End-use Properties: 1. PLA Compositions with Low Molecular Weight Ester-like Plasticisers and Related Performances." *Polymers for Advanced Technology* 19: 636–646. doi:10.1002/pat.1131.
- Murariu, M., A. D. S. Ferreira, M. Pluta, L. Bonnaud, M. Alexandre, and P. Dubois. 2008b. "Polylactide (Pla)-Caso₄ Composites Toughened with Low Molecular Weight and Polymeric Ester-like Plasticisers and Related Performances." *European Polymer Journal* 44: 3842–3852. doi:10.1016/j.eurpolymj.2008.07.055.
- Paydayesh, A., A. A. Azar, and A. J. Arani. 2015. "Investigation the Effect of Graphene on the Morphology, Mechanical and Thermal Properties of PLA/PMMA Blends." *Ciência e Natura* 37: 15–22.
- Petchwattana, N., W. Channuan, P. Naknaen, and B. Narupai. 2019. "3D Printing Filaments Prepared from Modified poly(lactic acid)/teak Wood Flour Composites: An Investigation on the Particle Size Effects and Silane Coupling Agent Compatibilisation." *Journal of Physical Science* 30: 169–188. doi:10.21315/jps.
- Petchwattana, N., and S. Covavisaruch. 2014. "Mechanical and Morphological Properties of Wood Plastic Biocomposites Prepared from Toughened poly(lactic acid) and Rubber Wood Sawdust (*Hevea brasiliensis*)." *Journal of Bionic Engineering* 11: 630–637. doi:10.1016/S1672-6529(14)60074-3.
- Petchwattana, N., P. Naknaen, J. Sanetuntikul, and B. Narupai. 2018b. "Crystallisation Behaviour and Transparency of poly(lactic acid) Nucleated with Dimethylbenzylidene Sorbitol." *Plastics, Rubber and Composites* 47: 147–155. doi:10.1080/14658011.2018.1447338.
- Petchwattana, N., and B. Narupai. 2019. "Synergistic Effect of Talc and Titanium Dioxide on poly(lactic acid) Crystallisation: An Investigation

- on the Injection Molding Cycle Time Reduction.” *Journal of Polymers and the Environment* 27: 837–846. doi:[10.1007/s10924-019-01396-0](https://doi.org/10.1007/s10924-019-01396-0).
- Petchwattana, N., and J. Sanetuntikul. 2018. “Static and Dynamic Mechanical Properties of poly(vinyl chloride) and Waste Rice Husk Ash Composites Compatibilized with γ -aminopropyltrimethoxysilane.” *Silicon* 10: 287–292. doi:[10.1007/s12633-016-9440-x](https://doi.org/10.1007/s12633-016-9440-x).
- Petchwattana, N., J. Sanetuntikul, and B. Narupai. 2018a. “Plasticization of Biodegradable poly(lactic acid) by Different Triglyceride Molecular Sizes: A Comparative Study with Glycerol.” *Journal of Polymers and the Environment* 26: 1160–1168. doi:[10.1007/s10924-017-1012-7](https://doi.org/10.1007/s10924-017-1012-7).
- Petchwattana, N., J. Sanetuntikul, P. Sriomreun, and B. Narupai. 2017. “Wood Plastic Composites Prepared from Biodegradable poly(butylene succinate) and Burma Padauk Sawdust (*Pterocarpus macrocarpus*): Water Absorption Kinetics and Sunlight Exposure Investigations.” *Journal of Bionic Engineering* 14: 781–790. doi:[10.1016/S1672-6529\(16\)60443-2](https://doi.org/10.1016/S1672-6529(16)60443-2).
- Prakash, M. O., G. Raghavendra, M. Panchal, S. Ojha, and P. S. C. Bose. 2018. “Influence of Distinct Environment on the Mechanical Characteristics of Arhar Fibre Polymer Composites.” *Silicon* 10: 825–830. doi:[10.1007/s12633-016-9536-3](https://doi.org/10.1007/s12633-016-9536-3).
- Rahman, M. A., D. De Santis, G. Spagnoli, G. Ramorino, M. Penco, V. T. Phuong, and A. Lazzeri. 2013. “Biocomposites Based on Lignin and Plasticized poly(l-lactic acid).” *Journal of Applied Polymer Science* 129: 202–214. doi:[10.1002/app.v129.1](https://doi.org/10.1002/app.v129.1).
- Satapathy, S., and R. V. S. Kothapalli. 2018. “Mechanical, Dynamic Mechanical and Thermal Properties of Banana fibre/recycled High Density Polyethylene Biocomposites Filled with Flyash Cenospheres.” *Journal of Polymers and the Environment* 26: 200–213. doi:[10.1007/s10924-017-0938-0](https://doi.org/10.1007/s10924-017-0938-0).
- Scatto, M., E. Salmini, S. Castiello, M. B. Coltelli, L. Conzatti, P. Stagnaro, L. Andreotti, and S. Bronco. 2013. “Plasticized and Nanofilled poly (lactic acid)-based Cast Films: Effect of Plasticiser and Organoclay on Processability and Final Properties.” *Journal of Applied Polymer Science* 127: 4947–4956. doi:[10.1002/app.38042](https://doi.org/10.1002/app.38042).
- Sommerhuber, P. F., J. Welling, and A. Krause. 2015. “Substitution Potentials of Recycled HDPE and Wood Particles from Post-consumer Packaging Waste in Wood-Plastic Composites.” *Waste Management* 46: 76–85. doi:[10.1016/j.wasman.2015.09.011](https://doi.org/10.1016/j.wasman.2015.09.011).
- Tajvidi, M., and A. Takemura. 2010. “Thermal Degradation of Natural Fibre-reinforced Polypropylene Composites.” *Journal of Thermoplastic Composite Materials* 23: 281–298. doi:[10.1177/0892705709347063](https://doi.org/10.1177/0892705709347063).
- Teymoorzadeh, H., and D. Rodrigue. 2015. “Biocomposites of Wood Flour and Polylactic Acid: Processing and Properties.” *Journal of Biobased Materials and Bioenergy* 9: 1–6. doi:[10.1166/jbmb.2015.1510](https://doi.org/10.1166/jbmb.2015.1510).
- Wang, Y., R. Qi, C. Xiong, and M. Huang. 2011. “Effects of Coupling Agent and Interfacial Modifiers on Mechanical Properties of poly (lactic acid) and Wood Flour Biocomposites.” *Iranian Polymer Journal* 20: 281–294.
- Xu, Y. Q., and J. P. Qu. 2009. “Mechanical and Rheological Properties of Epoxidised Soybean Oil Plasticized poly(lactic acid).” *Journal of Applied Polymer Science* 112: 3185–3191. doi:[10.1002/app.29797](https://doi.org/10.1002/app.29797).